HANDBOOK OF GRANULAR MATERIALS

edited by

Scott V. Franklin

Mark D. Shattuck

CRC Press
Taylor & Francis Group

HANDBOOK OF
GRANULAR MATERIALS

HANDBOOK OF **GRANULAR MATERIALS**

edited by

Scott V. Franklin

Mark D. Shattuck

CRC Press
Taylor & Francis Group
Boca Raton London New York

CRC Press is an imprint of the
Taylor & Francis Group, an **informa** business

CRC Press
Taylor & Francis Group
6000 Broken Sound Parkway NW, Suite 300
Boca Raton, FL 33487-2742

Version Date: 20160120

International Standard Book Number-13: 978-1-4665-0997-9 (eBook - PDF)

Visit the Taylor & Francis Web site at
http://www.taylorandfrancis.com

and the CRC Press Web site at
http://www.crcpress.com

SVF dedicates this book to his wife, Merrie, and sons Maxwell, Gabriel, and Harry, whose tolerance and support were instrumental to completing this work.

MDS dedicates this book to his children Sarah and Eli and his wife Dianna, and thanks them for their patience and support during the entire process.

Contents

Preface

This book was assembled for many reasons. The explosion of research over the last two decades has greatly advanced our understanding of granular materials, to the point where some broad themes can now be stated with some confidence. Additionally, the experimental, theoretical, and computational methods of inquiry have all seen significant development, both individually and in relation to one another. This book attempts to tie these developments together, providing guidance on how to conduct research in granular materials and also promising directions for new research.

The book is organized into three sections. Chapters 2 through 5 cover the various methods that contemporary researchers use to investigate granular materials. Chapters 6 through 10 delve into broader themes of investigation, focusing on results, not methodology. Finally, Chapters 11 through 13 describe three systems: suspensions, emulsions and foams, and colloids that can be considered as extensions of granular media. Many of the same approaches are used in these systems, although the microscopic nature often requires innovative experimental techniques.

The methods section begins with chapters on computational and experimental methods and techniques. While no review can be comprehensive, these chapters aim to provide the reader with an understanding sufficient to serve as the foundation for future study. Theoretical approaches are varied, and so we have chosen two kinetic theory and statistical approaches that are both broad enough to be applicable in a number of different situations and make specific predictions and advances so as to be widely relevant.

Recent research has been rather arbitrarily divided into static/quasi-static and dynamic effects. Chapter 6 describes computational research on static packings, while Chapter 7 describes the mechanical response of experimental packings to very small disturbances. The use of photoelastic material to directly visualize chains of force throughout the granular material has contributed much to our understanding of the response, and so Chapter 7 includes a description of this technique. The remaining chapters deal with dynamic features. Chapter 8 describes granular shear in simple systems, followed by a description of an elegant set of experiments and theory on granular avalanches, a system of critical relevance to natural phenomena such as avalanches, landslides, and earthquakes. Finally, the tendency of mixtures of two (or more) different materials to segregate under shear flows, covering both shaken and rotating systems, is discussed in Chapter 9.

The final section contains chapters that are extensions of granular systems: suspensions, emulsions and foams, and colloids. Each of these deals with various limiting cases of granular systems, for example, the absence of friction or the importance of Brownian motion. While the length and time scales of the phenomena may vary widely, the picture that emerges is complementary to that of canonical granular systems.

A beginning researcher might start, therefore, by choosing three appropriate chapters: a method, a theme, and an extension. In this way, the student learns the how, what, and why of their project. This should not be seen, of course, as implying that the remaining chapters would not in themselves be valuable, and both the editors of this book have learned a great deal in the process of reading the chapters.

Acknowledgments

The editors personally thank each of the authors who have contributed to this book. Their dedication and care come through clearly in every chapter, and the responsibility for any errors, typos, or other confusions rests solely on us. We also thank Taylor & Francis Group for suggesting this project and for their patience in its assembly.

I (Franklin) acknowledge support from the American Chemical Society's Petroleum Research Fund (PRF #51438-UR10) and the National Science Foundation (CBET #1133722). I also thank my coeditor, Mark Shattuck, whose knowledge and vision were invaluable.

I (Shattuck) acknowledge support from the National Science Foundation (DMR PREM Grant No. DMR0934206 and CBET-0968013) and from the Kavli Institute for Theoretical Physics through the National Science Foundation under Grant No. NSF PHY11-25915. I thank Scott Franklin for his enthusiasm and guidance.

Editors

Scott V. Franklin earned his bachelor's degree from the University of Chicago, Chicago, Illinois, in 1991 and his PhD from The University of Texas in Austin, Austin, Texas, in 1997. In 2000, after a two-year National Science Foundation postdoctoral fellowship in physics education research, he joined the faculty at Rochester Institute of Technology. He currently maintains a lab that focuses on experimental and computational investigations of granular and other complex materials. Recent interests of the lab include rodlike and other materials that, due solely to particle shape, can maintain a solid-like rigidity.

Mark D. Shattuck earned his bachelor's degree and MS in 1987 and 1989 from Wake Forest University, Winston-Salem, North Carolina, and his PhD from Duke University, Durham, North Carolina, in 1995. He held postdoctoral fellowships in medical physics at Duke University and in granular physics at the University of Texas before joining the faculty of The City College of New York in the Benjamin Levich Institute in 2000, where he performs experimental and computational research in soft condensed matter and granular materials. He has 15 years of experience and more than 25 publications in studies of particulate systems, and has developed a number of novel imaging and production techniques for particulate systems. He is an editor for the research journal *Granular Matter* and served on the Publication Oversight Committee of the American Physical Society for five years (with two as chair). He is a founding organizer of the annual regional meeting Northeastern Granular Materials Workshop.

Contributors

Robert P. Behringer
Department of Physics
Center for Nonlinear and Complex Systems
Duke University
Durham, North Carolina

Bulbul Chakraborty
Martin A. Fisher School of Physics
Brandeis University
Waltham, Massachusetts

Karin A. Dahmen
Department of Physics
University of Illinois at Urbana Champaign
Urbana, Illinois

Scott V. Franklin
Department of Physics
Rochester Institute of Technology
Rochester, New York

Piotr Habdas
Department of Physics
Saint Joseph's University
Philadelphia, Pennsylvania

Kimberly M. Hill
Department of Civil, Environmental and Geological Engineering
University of Minnesota Twin Cities
Minneapolis, Minnesota

James T. Jenkins
School of Civil and Environmental Engineering
Cornell University
Ithaca, New York

Arshad Kudrolli
Department of Physics
Clark University
Worcester, Massachusetts

Jeffrey F. Morris
Benjamin Levich Institute
and
Department of Chemical Engineering
The City College of New York
New York, New York

Corey S. O'Hern
Department of Mechanical Engineering and Materials Science
and
Department of Applied Physics
and
Department of Physics
Yale University
New Haven, Connecticut

Ashish V. Orpe
Chemical Engineering Division
National Chemical Laboratory
Pune, India

Andreea Panaitescu
Department of Physics
Clark University
Worcester, Massachusetts

Mark D. Shattuck
Benjamin Levich Institute
and
Department of Physics
The City College of New York
New York, New York

Brian P. Tighe
Process and Energy Laboratory
Delft University of Technology
Delft, the Netherlands

CHAPTER 1

Introduction

Scott V. Franklin and Mark D. Shattuck

CONTENTS

This introduction discusses historical topics of personal interest. The topics chosen are not in any way comprehensive, nor motivated by anything other than models, theories, and experiments that I found particularly enlightening. The reader is enthusiastically referred to the many existing articles and books that also give introductions to granular materials, particularly in areas with which I am less familiar (e.g., engineering, for which readers are referred to the extensive literature, e.g., [15,25]). The personal retrospective gives an emphasis to simple statistical explanations, an aesthetic property that has proven exceptionally useful for my own study of granular materials. The section concludes with a review of my personal area of research: geometrically cohesive materials.

1.1 Statistical Models

1.1.1 Avalanches, Angles of Repose, and Self-Organized Criticality

In 1987, Bak et al. [3] proposed the idea of self-organized criticality (SOC) to explain the near ubiquity of noise with a $1/f$ power spectrum, particularly in systems where such noise might originate from mechanisms with spatial extents. The power-law scaling implies the absence of a fundamental length scale, and so the challenge was to devise a system that evolved to a critical state without such a length. For their system, they chose a simplified model of granular avalanching, one whose analogs have been the focus of subsequent research to this day [28,36,42]. One attractive feature of the model is its computational simplicity; a reader with basic programming skills can likely reproduce the fundamental result in only a few hours.

The model begins with a surface profile on a discretized lattice $z(i,j)$, with z representing the height of the granular pile. A site is chosen at random and the height increased by 1, representing the addition of a single grain to the pile. Rules then redistribute the material when the height exceeds a critical value. In the original SOC paper, if the absolute height exceeded a critical value (K), then an avalanche delivered 1 grain to each of four neighbors (assuming a square lattice indexed by i and j):

$$z(i,j) > K \Longrightarrow \quad z(i,j) \to z(i,j) - 4 \tag{1.1}$$

$$z(i \pm 1, j) \to z(i \pm 1, j) + 1 \tag{1.2}$$

$$z(i, j \pm 1) \to z(i, j + 1) + 1 \tag{1.3}$$

Subsequent models [8] considered the difference in height between a point and its neighbors, with material flowing "downhill" when the height at any point exceeds that of its neighbors by a critical amount. While the specific nature of the redistribution is not important, the key point is that the transfer of material from one point to another can induce subsequent transfers, representing a broad, spatially extended event. Events can be quantified in a number of ways: by the total number of grains that moved from one position to another, by the number of sites involved in a transfer, or by the spatial geometry of the involved sites. Bak et al. found that, for a variety of system sizes in two and three dimensions, the distribution of cluster sizes is a power-law with exponent −1, indicating the absence of a characteristic event size. Because this occurred for a variety of initial conditions and system dimensions and sizes, Bak et al. asserted it was a fundamental characteristic of the system that was "self-organized" to the critical state.

Following almost immediately were two experiments of Jaeger et al. [22] on the angle of repose of a granular pile. The first reproduced the model of Bak et al., adding particles at random to a box of sand with one open side. The second consisted of a thin drum, partially filled with material, that rotated slowly. Jaeger et al. measured the capacitance across the system, which depends on the amount of (dielectric) material in that volume and is sensitive enough to capture changes involving even just a few grains (glass beads of diameter .07–.5 mm). This method was subsequently used in a number of experiments that measured the evolution of packing fraction of both spheres [24,33] and rods [48] in response to tapping.

Contrary to the prediction of self-organized criticality, Jaeger et al. observed the distribution of event size to be independent of frequency, which could be explained as the superposition of spatially extended events that occupy a very narrow range of time scales. Jaeger et al. then considered whether the discrepancy could be explained by the non-unique nature of the dynamic angle of repose. Bak et al. had assumed that avalanches begin as soon as the local angle exceeded a single value θ_r. Jaeger et al. found instead that the angle at which flow started typically exceeded θ_r by a small amount, which was related to the need for the particles to dilate slightly in order to flow. By adding energy to the pile through small vibrations (which dilated the pile and facilitated flow), Jaeger removed the excess angle from the experiment but still did not capture $1/f$ power-law scaling.

Despite the apparent quantitative failure of self-organized criticality, the model spurred a lasting interest in granular avalanching and the close study of event size distribution. Indeed, an entire chapter of this book—Chapter 9—deals with contemporary theories of avalanches.

1.1.2 Force Chains and the q Model

When forces are applied to a granular system, the discrete nature of particles, coupled with the random distribution in space, causes the force to be concentrated into "force chains," with significant load being borne by a relatively small number of particles, while many particles feel comparably small forces. A common technique to visualize this is the use of photoelasticity, where elastic deformations of a material rotate the polarization vector of light passing through the particle in both two (e.g., [17,21]) and three [19] dimensions. Viewed between two polarizers oriented 90° to one another, an unstressed particle will appear dark (since the second polarizer completely blocks the light) while the stressed particles appear bright. An example is shown in Figure 1.1, and more details are given in Chapters 3 and 7.

The mechanism by which forces can grow large is illustrated by the simple picture in Figure 1.2. Two grains support the weight of a single grain immediately above. Because the grains are offset by an angle θ, the force on each grain must be $F = W/(2\sin\theta)$ in order to balance the forces. As θ becomes small, this force becomes quite large. This magnification has significant practical consequences, as containers must be constructed to support significant lateral forces that arise.

An early attempt to explore the inhomogeneity of the force distribution was proposed by Liu et al. [19] and Coppersmith et al. [10], and termed the "q" model. While no longer the dominant paradigm for understanding force chains, its status as an early appeal to random walk statistics left a lasting mark on subsequent theories. In particular, it bears striking similarity to a later work on jamming of flow through conical hoppers in two (c.f. To et al. [45]) and three [53,54] dimensions and anisometric wedge hoppers [41].

An important result was to identify the power-law distribution of Bak's SOC model as a rare special case, with more physically realistic situations resulting in

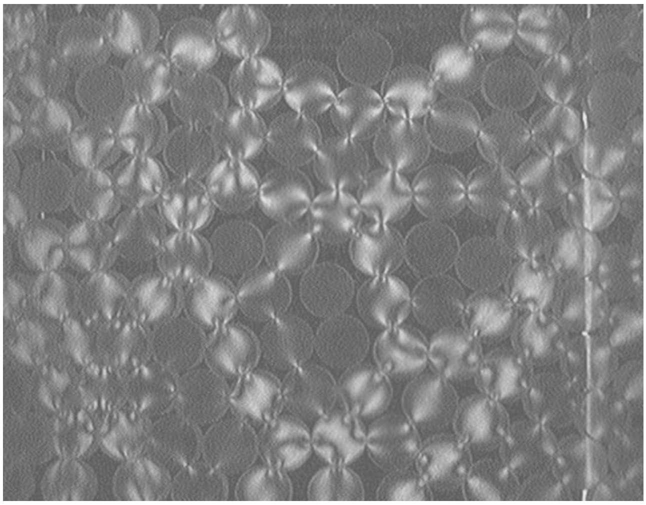

Figure 1.1 1 cm diameter photoelastic disks in a thin channel, compressed from the top. The disks are between crossed linear polarizers, and stress-induced birefringence results in the picture shown: the white streaks are force chains.

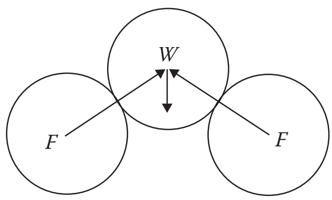

Figure 1.2 Simple illustration of two lower grains supporting a third, with weight W. Because the contact forces are at an angle with respect to gravity, they must be larger in order for their vertical components to support the upper grain's weight.

qualitatively different scalings. The model assumes a regular lattice of beads, with each row supporting the weight of the row immediately above it. The randomness of a real pile is captured by the rule that a particle distributes a random fraction of its load to each of its neighbors below. The fraction from the ith particle in a given layer to the jth particle in the layer below is labeled q_{ij}, and the total weight on the jth particle is therefore a sum over the i contacting particles from above. This leads to a recursive relation for the load on the jth particle in layer D:

$$w(D+1,j) = 1 + \sum_i q_{ij}(D)w(D,i).$$

The factor of 1 represents the weight of the particle itself, whereas the sum is over all the contacting neighbors from above, each supporting their own load $w(D,i)$ and distributing the fraction $q_{ij}(D)$ to the particle in question. The critical feature of the model is that the distributing fractions q_{ij} are *completely uncorrelated* from one another; in this way, the problem takes on the form of a random walk.

Coppersmith et al. identified two distinctly different results from this model. The simplest case, which they termed the critical $q_{0,1}$ limit, involved particles distributing either all or none of their load to a particular neighbor below. That is, the random variables q_{ij} were either 0 (no load transmitted) or 1 (all load transmitted). This is formally equivalent to a discrete random walk, with paths from particles above coalescing as they move downward. In this limit they did indeed find a power-law scaling of the weight distribution function with depth, with

$$Q_D(w) \propto D^{-a}.$$

When the random values q_{ij} were allowed to assume values other than 0 and 1, however, thus resembling a random walk with a distribution of step size, the results were qualitatively different. Allowing the distribution parameters to vary between 0 and 1 (while summing to 1 to conserve mass) was a much more physically realistic situation, more closely modeling the random packing of actual materials. In these cases, the distributions did not show a power-law scaling, decaying much more rapidly (usually exponentially). Coppersmith et al. presented both numerical and mean-field theory results to support this finding, and the agreement with direct simulations of sphere packings and experiments cast further doubt as to the applicability of self-organized criticality as the mechanism by which sandpiles form and collapse.

1.2 Flow through Hoppers

The flow of granular material through hoppers is also is well-captured by random walk-like models that, in their assertion of uncorrelated events, bear a striking similarity to that proposed by the q-model. Hopper and funnel flow have obvious industrial importance, and physicists and engineers have focused on both the flow rate through a hopper and the probability with which particles clog at the exit aperture. The latter question, intimately connected with the theory of jammed systems, presents an outstanding problem that involves two- and three-dimensional experiments and particulate and continuum theories. Clogging of particles at a hopper outlet affects a wide range of industrial processes that transport granular media through pipes, silos, and hoppers [7,12]. While early research focused on the steady-state flow rate [5], more recent attention has turned to the probability that flow stops, that is, the transition to the jammed state. Here I will describe several studies that each take a slightly different approach to understanding clogging in hoppers. An ultimate unifying theory is tantalizingly close.

1.2.1 Two-Dimensional Hoppers and Mean Field Statistical Theories

In 2001 and 2002, To et al. published a series of articles [44–46] that described a simple two-dimensional experiment and an elegant statistical theory that captured the clogging of disks flowing through a 2D hopper. The experiments allowed disks of uniform radius to flow through the hopper until a clog occurred and, when flow had stopped, took a picture of the arch that formed at the exit. They varied the size of the aperture (measured in particle diameters) and angle of the hopper side-walls. The critical question was a statistical description of the clogging arch and, if possible, an explanatory theory.

Experimentally To et al. measured an expected monotonic decrease in probability to clog as a function of aperture diameter and corresponding increase in the average number of particles that took part in a clogging arch. The clogging probability was simply the fraction of experiments that experienced a clog; given the finite system size (200 particles), it was possible for all the particles to flow through the aperture. Data from To's 2002 paper showing the probability approaching zero as the aperture width approaches five particle diameters are shown in Figure 1.3. The probability for the particles to clog drops sharply as the aperture grows larger than three particle diameters, and is practically zero (meaning the hopper empties completely) when the aperture is five diameters in size.

The two-dimensionality of the system allows an explicit enumeration of all the possible configurations of a jamming arch. In some ways, this presaged a similar undertaking of O'Hern et al. [16,51] to count all of the different configurations of N particles that occupy the same packing fraction and Franklin et al. [41] to investigate jamming in anisometric (wedge) hoppers. The experimental observations

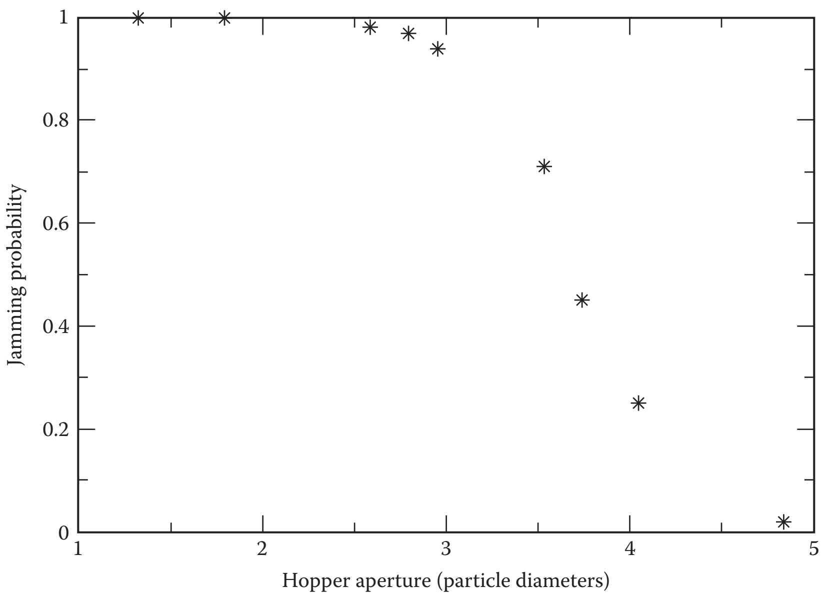

Figure 1.3 The experimental probability for a two-dimensional hopper containing 200 particles to clog as a function of hopper aperture (measured in particle diameters). Hoppers with apertures less than three particle diameters in size almost always clog; hoppers with apertures greater than four particle diameters almost never do. (Data adapted from To, K. et al., *Phys. Rev. Lett.*, 86, 71, 2001.)

can be reproduced by applying a *restricted random walk model* that assumes that a disk's location is uncorrelated with respect to those of its neighbors. For an arch to form, three constraints/conditions must be met:

- The angle θ_i between a point connecting the centers of mass of neighboring disks must be between $\pm\pi/2$. This requires the arch to continually progress across the space, i.e., disk "2" is always to the right of disk 1.
- Arches must be convex (down). That is, the angle between two disks must be smaller than the angle between the two previous disks.
- The horizontal span of the arch must exceed the aperture width (obvious).

Additionally, to enable the theoretical treatment the disks are assumed hard, so the distance between two disks in contact is the particle diameter. Given these constraints, the probability of n disks to span an arch of width x is given by

$$P_n(x) = \int_{-\pi/2}^{\pi/2} d\theta_2 \int_{-\pi/2}^{\theta_2} d\theta_3 \ldots \int_{-\pi/2}^{\theta_{n-1}} d\theta_n \, \delta\left(d - 1 - \sum_{i=2}^{n} \cos\theta_i \right) \tag{1.4}$$

From Equation 1.4, To calculated the probability that n particles would randomly configure to span a horizontal distance x, reproduced for arches of up to nine particles in length in Figure 1.4a. For a fixed aperture width D, the probability of jamming with an arch of n particles is just the cumulative sum of the individual probabilities of forming an arch with length greater than D, that is,

$$J_n(D) = \int_{D}^{\infty} P_n(x)\, dx. \tag{1.5}$$

In determining the total probability of a jam, regardless of arch geometry, To et al. again assumed that all possible arches were equally probable and considered the normalized sum over all arch sizes. To properly normalize the contribution from a particular geometry, they calculated the fraction of jamming ($x > D$) arches with n particles compared to the total number of jamming arches:

$$g_d(n) \equiv \frac{J_n(D)}{\sum_n J_n(D)}.$$

The total jamming percentage is then

$$J(D) = \sum_n g_d(n) J_n(d).$$

This integrated sum is shown in Figure 1.4b. The close agreement between experiment and model gives strong support to the idea that particles in flow sample with equal probability the entire configuration space and that, at least in two dimensions, it might be possible to write down closed forms for the mechanically stable configurations.

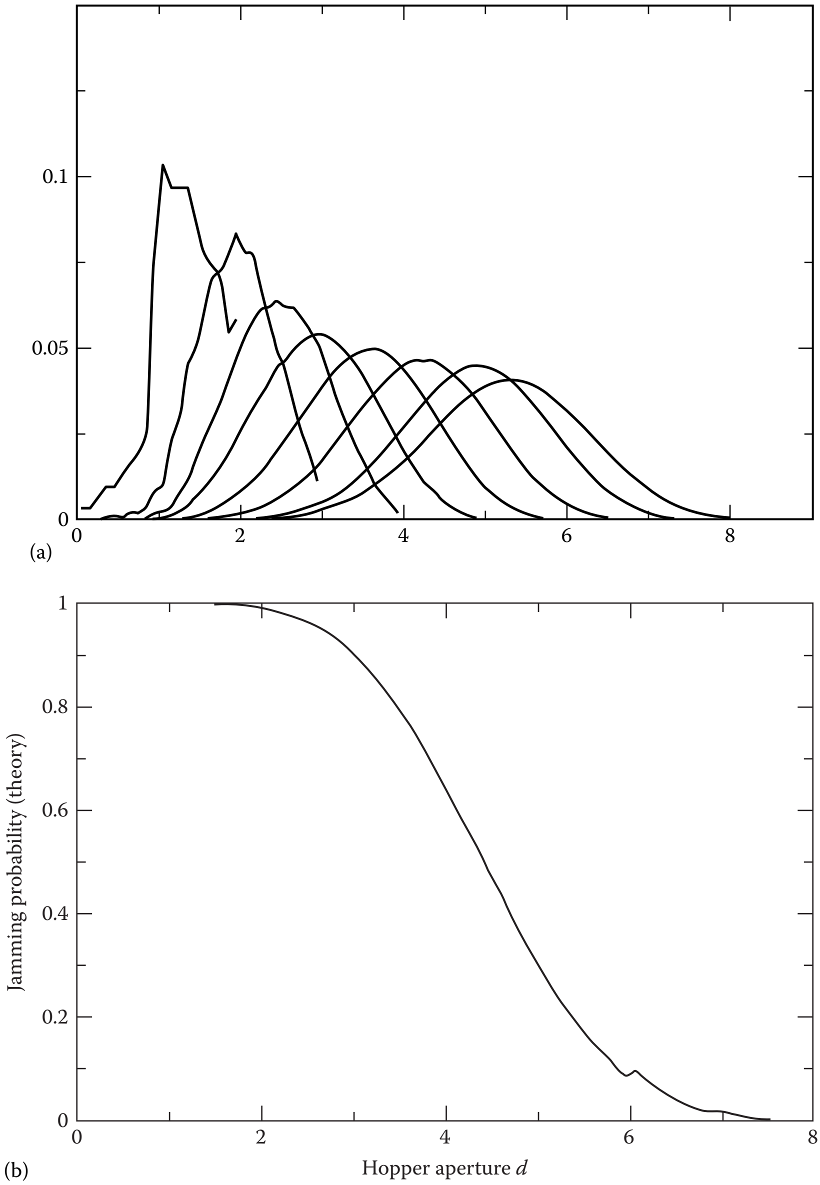

Figure 1.4 (a) Probability for an arch of N particles to span an aperture of a distance d for $N = 2, 3, \ldots 9$. (b) Theoretical jamming probability as a function of aperture width calculated as in Equation 1.5. (Figures recreated after To, K. et al. *Phys. Rev. Lett.*, 86, 71, 2001.)

1.2.2 Three-Dimensional Hoppers: Cones and Wedges

Where To et al. studied the likelihood of a specific jamming configuration, Zuriguel et al. [53,54] investigated the amount of material that exited a hopper before the jam occurred. A conical hopper filled with spherical particles emptied onto a scale, which recorded the flow of material. When the drainage stopped, a puff of air broke apart the arch at the entrance and flow resumed. The event-size distribution was observed to have a broad exponential tail, which can be explained with the following simple uncorrelated statistics model. The probability of a particle (or group of particles) to flow through without jamming is modeled as p, and is independent of whether neighboring (or prior) particles have flowed. Thus the probability of exactly N particles (or groups) to exit before the system jammed is

$$P(N) = N^p(1-p)$$

the factor of $(1-p)$ indicating that the $N+1$th particle does, in fact jam. This can be rewritten as

$$P(N) = (1-p)\exp(N\log p)$$

and, since $p < 0 \Longrightarrow \log p < 0$, the large N limit goes as

$$P(N \gg 1) \sim \exp[-\,|\log p\,|\,N].$$

The argument and scaling are essentially unchanged if, instead of a single particle, p refers to the probability for a correlated group of particles to exit.

More recently, Janda et al. [23] connected the probability of forming an arch of specific size with the exit mass probability distribution function and also investigated how the mean flow $\langle N \rangle$ scaled with aperture diameter. A key finding was the absence of a critical aperture size above which the mean flow diverges. Rather, $\langle N \rangle$ grows with aperture diameter D as $\langle N \rangle \propto \exp[D^2]$.

Zuriguel's work focused on conical hoppers, with a circular aperture. More recently, Saraf et al. investigated the flow of round particles (acrylic spheres) through a wedge hopper with a rectangular aperture. In marked contrast with the data from conical hoppers, Saraf et al. found the probability for N particles to exit the hopper before jamming to have a broad power-law decay with exponent $\alpha = -2$, shown in Figure 1.5. After an initial plateau, the distribution falls off as a power-law with $P(N) \sim N^{-2}$.

Both the exponential tail seen in conical hoppers and the power-law distribution from wedge hoppers can be captured in a single model that postulates correlated string-like dynamics over a length scale comparable to the smallest length scale of the hopper. The probability for a correlated string of particles to exit p is now a function of the string orientation θ, as strings aligned along the length of the aperture have a high probability of passing through while those aligned across the width have a smaller probability. The experimentally observed distribution function is an average over the range of individual string exit probabilities.

Similar to models discussed previously, the strings are assumed to evenly sample all orientations and be uncorrelated with the orientation of previous (or subsequent) strings passing through the aperture. Calculating these averages,

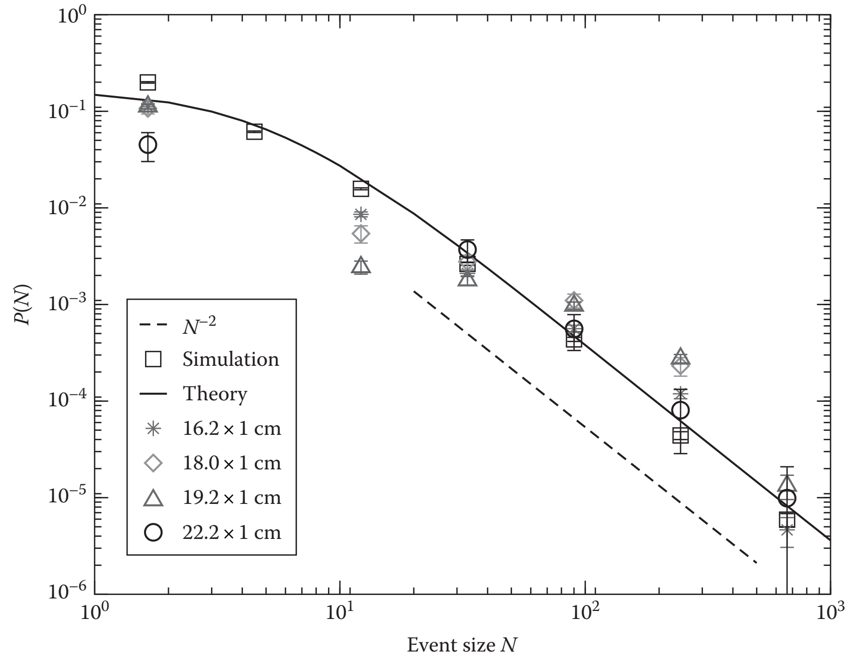

Figure 1.5 The probability for N particles to exit a wedge hopper has a broad power-law tail with $P(N) \sim N^{-2}$ (dashed line), seen in experiments, Monte Carlo simulation, and analytic theory. This is in distinct contrast to the distribution function found in conical hoppers, which decays exponentially. Shown are distribution functions for experimental hoppers of lengths $L = 16.2$–22.2 cm. Simulation and theory assume $n_c = 3$ adjacent, statistically independent cells. (From Saraf, S. and Franklin, S.V., *Physical Review E*, 83(3), 030301, March 2011.)

therefore, bears a striking resemblance to To's mean field model. The limits of the exit probability for strings parallel and perpendicular to the aperture are p_z and p_x and the uniform distribution of exit probability between $p_x < p < p_z$ takes the form

$$O(p) = \frac{\theta(p - p_x)\theta(p_z - p)}{p_z - p_x}. \tag{1.6}$$

$\theta(p - p_x)$ and $\theta(p_x - p)$ are Heaviside step functions, and $p_z - p_x \equiv \Delta p$ is a normalizing factor. The probability for exactly N strings to exit now requires the averaging over all allowable exit probabilities with the integral

$$\langle P(N) \rangle = \int_{p_x}^{p_z} p^N (1 - p) O(p) dp. \tag{1.7}$$

For an isometric (round) aperture, the exit probability is independent of orientation: $p_z = p_x$. The orientational probability $O(p)$ in Equation 1.7 is functionally equivalent to a Dirac delta function at p_x, and the event size probability

$$\langle P(N) \rangle \approx \int p^N (1-p)\delta(p-p_x)\, dp = p_x^N (1-p_x) \tag{1.8}$$

captures the exponential decay seen in conical hoppers.

The assumption that strings assume all orientations with equal likelihood allows one to calculate the indefinite integral of Equation 1.7

$$\int p^N (1-p) O(p)\, dp = \frac{1}{\Delta p}\left[\frac{p^{N+1}}{N+1} - \frac{p^{N+2}}{N+2}\right], \tag{1.9}$$

For $p < 1$, the result is a power-law, scaling as $1/N$, with an exponential cutoff (since the term in the numerator is $p^N = \exp[N \ln p]$). As $p \to 1$ the exponential cutoff occurs at larger and larger N, however, eventually disappearing when $p = 1$.

Physically, $p \to 1$ means that a string of particles has no probability of forming an arch and jamming at the hopper aperture, which implies that the aperture is longer than the string length. In this limit of $p = 1$, Equation 1.7 integrates to

$$P(N) = \frac{1}{1-p_x}\left[\frac{1}{(N+1)(N+2)} + \frac{p_x^{N+1}}{N+1} - \frac{p_x^{N+2}}{N+2}\right] \tag{1.10}$$

and $P(N \to \infty) \propto 1/N^2$. This power-law scaling explains the experimental findings of Figure 1.5.

The probability distribution for several values of p_z is shown in Figure 1.6. The exponential cutoff is seen to occur for larger and larger values of N as p_z approaches 1. It is natural to assume that transition from exponential to power-law distribution occurs as the aperture's long length approaches the length scale over which correlated motion occurs [9].

Saraf et al. also showed how the model could be extended to still longer apertures to perhaps capture the spatially and temporally inhomogeneous flow through anisometric hoppers. The aperture is modeled as a series of n_c adjacent "cells," each of length equal to the granular string length. The probability for n_i particles to exit the ith cell is given by Equation 1.10 and, following this chapter's theme, the probabilities for different cells were assumed to be statistically independent. The average exit mass probability distribution is calculated by summing over all the different ways that N particles can exit n_c cells:

$$\langle P(N) \rangle = \sum_{n_1, n_2, \ldots = 0}^{N} \prod_{i=1}^{n_c} P(n_i)\delta\left(N - \sum_{i=1}^{n_c} n_i\right), \tag{1.11}$$

where the delta function forces the sum of the particles exiting the individual cells to total N: $n_1 + n_2 + \cdots = N$. Interested readers are referred to [41] for additional details and results.

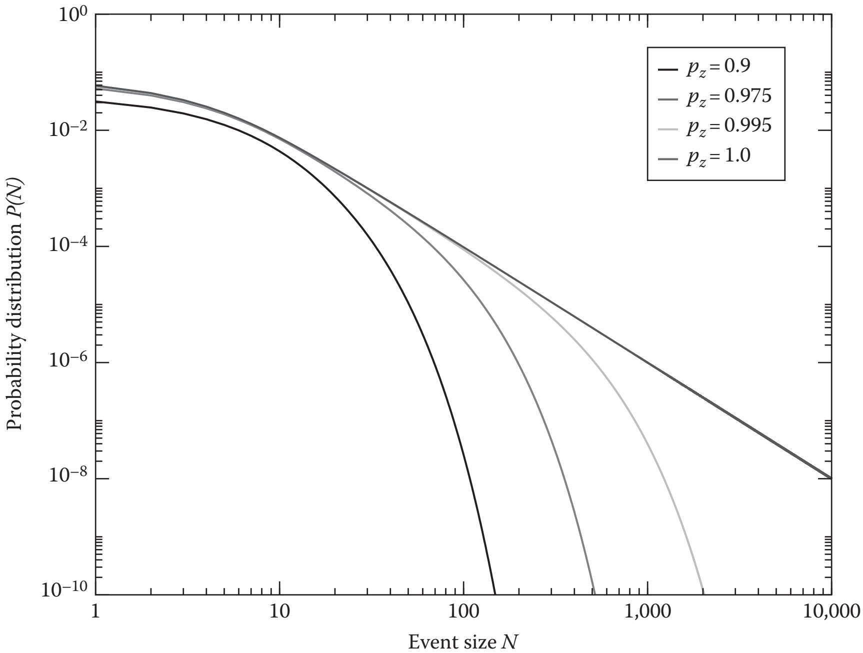

Figure 1.6 Evaluation of Equation 1.7 for values of p_z approaching 1. When $p_z < 1$ the curve has a power-law tail with an exponential cutoff. At $p_z = 1$ the exponential cutoff disappears leaving behind only the power-law tail. (From Saraf, S. and Franklin, S.V., *Physical Review E*, 83(3), 030301, March 2011.)

1.3 Irregularly Shaped Granular Materials

I conclude the section with a review of work on radically aspherical materials, primarily long, thin rods, and U-shaped staples. I will focus on statistics of the packings, which can demonstrate correlations that violate the mean-field assumptions of the previous sections, and the peculiar rigidity that particle entanglement can cause.

1.3.1 Packing of Long, Thin Rods

The packing of long, thin rods of large aspect ratio ($\alpha \equiv L/D > 10$) can result in piles that are both remarkably stable and yet form very low packing fractions. Philipse [37,38] was the first to study the solid "plug like" behavior that rods with aspect ratio above $\approx$35 displayed when poured from a container and gave a simple geometric argument, the random contact model (RCM), to explain the very low packing fractions. The model rests on a mean field assumption that particle orientations are uncorrelated and sample equally all possible orientations and is thus thematically consistent with the models discussed earlier in this chapter. Coupled with this is the idea of *excluded volume* the volume in space forbidden to another particle due to the existence of another. Onsager [35] had in fact calculated this excluded volume for spherocylinders (cylinders of length L and diameter D with two hemispherical end caps) in his study of phase transitions in colloidal suspensions, finding it to be

$$V_{ex} = \frac{\pi}{2}L^2D + 2\pi D^2L + \frac{4}{3}\pi D^3.$$

If orientations are uncorrelated then each particle can be assumed to occupy a volume equal to its excluded volume and the pile number density is inversely proportional to the excluded volume and proportional to the average number of contacts per particle $\langle c \rangle$:

$$N = \frac{2\langle c \rangle}{V_{ex}},$$

where the factor of 2 occurs because each contact involves two particles. The packing fraction is the product of the number density and particle volume ($V_{part} = (\pi/6)D^3 + (\pi/4)D^2L$) and, for large aspect ratios, does indeed scale inversely with aspect ratio, confirming the model's assumptions. Subsequent experiments by Desmond and Franklin [11] found it necessary to keep the higher order terms in the excluded volume fraction for aspect ratios from 5 to 50 in a variety of cylinder packings, but the model otherwise explained 3D packings quite well.

The mean-field assumption of random contacts breaks down, however, for 2D piles formed under gravitational collapse, as most interactions between particles bring about alignment and there is not sufficient entanglement to prevent this from occurring. This was demonstrated in experiments by Stokely et al. [43], who formed 2D piles under gravity and compared both the packing fraction and orientational correlations with the mean-field predictions.

The 2D excluded area is, to first order, $A_{excl} = (2/\pi)L^2$ [4] and the predicted number density as a function of aspect ratio α therefore

$$N(L) = \frac{2\langle c \rangle}{(2L^2/\pi)} = CL^{-2}.$$

Figure 1.7 shows that the number density does indeed fall off as L^{-2} for large L, but the prefactor is significantly larger than that predicted by the RCM. Piles are ≈33% more dense than predicted, with particles occupying ≈33% less area than in an isotropic distribution.

The increased packing results from particle alignment, which can be seen in correlations between particle orientations. Figure 1.8 shows the angular orientation correlation function

$$\tilde{Q}(r) = \langle \cos(2\Delta\theta_{ij}) \rangle, \tag{1.12}$$

with $\Delta\theta_{ij}$ the difference in angle between particles i and j and the average over all particles whose centers of mass separation is between r and $r + \delta r$. Two particles whose centers of mass are quite close must be aligned and so $\tilde{Q}(r \to 0) \to 1$. Once particle centers of mass are separated by more than one particle length L they can in principle assume any relative orientation and so $\tilde{Q}(r \to \infty) \to 0$.

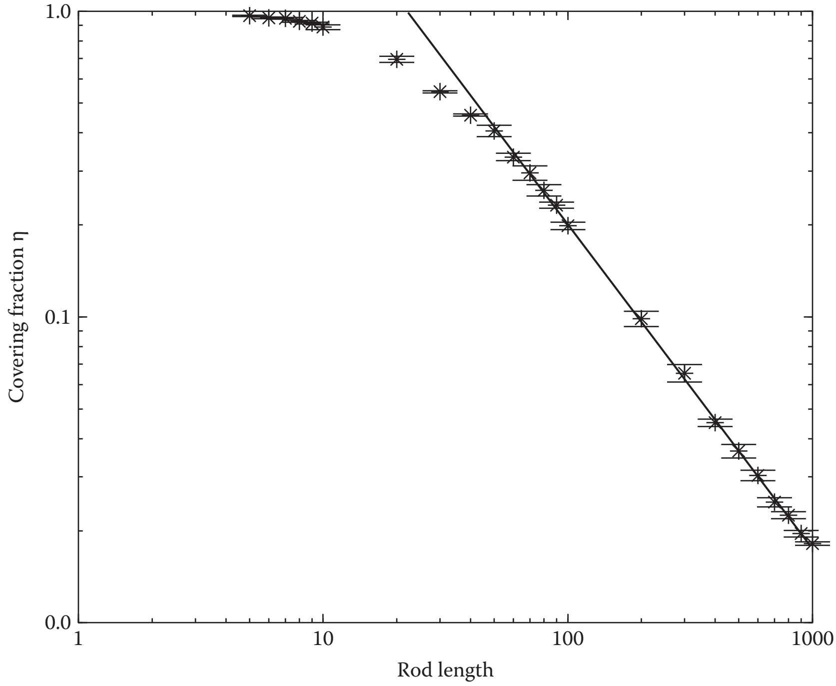

Figure 1.7 Log-log plot of packing fraction ϕ as a function of particle aspect ratio α. Data are grouped by constant dimensionless container diameter $\tilde{D} \equiv D/L$. With the exception of a few points at low $\tilde{D}$ (where significant particle alignment occurs), the data are well fit by a mean-field theory with only one free parameter.

Figure 1.8 shows the $\tilde{Q}(r)$ distribution that results from averaging Equation 1.12 over all allowable angles, assuming all are sampled equally, as well as that obtained from Monte Carlo simulations and experimental piles. The theoretical $Q(r)$ begins at 1 and rapidly decays to zero as $r \to 1$, as it must. Both the experimental and simulated piles, however, show significantly greater correlation between neighboring particles, seen in the divergence from the analytic line for $r/L > 0.5$ (between the dashed lines), and reach a nonzero asymptote once particles are separated by more than two particle lengths. This nonzero asymptote indicates a long-range ordering, with particles preferring to align with the container walls. This demonstrates the deviation from uncorrelated behavior assumed in most of the models discussed in this section and explains the enhanced packing fraction observed in experiment.

1.3.2 Geometric Cohesion in Granular Materials

Radically aspherical particles may display a cohesion brought about by entanglement. Figure 1.9 shows a pile of rods (aspect ratio 48) suspended by a single point force applied to the bottom. In this case, the force is applied by a small sphere connected to a string passing through the pile (which can be seen exiting the top of the pile) and suspended from above. The pile was formed in a large cylinder and then

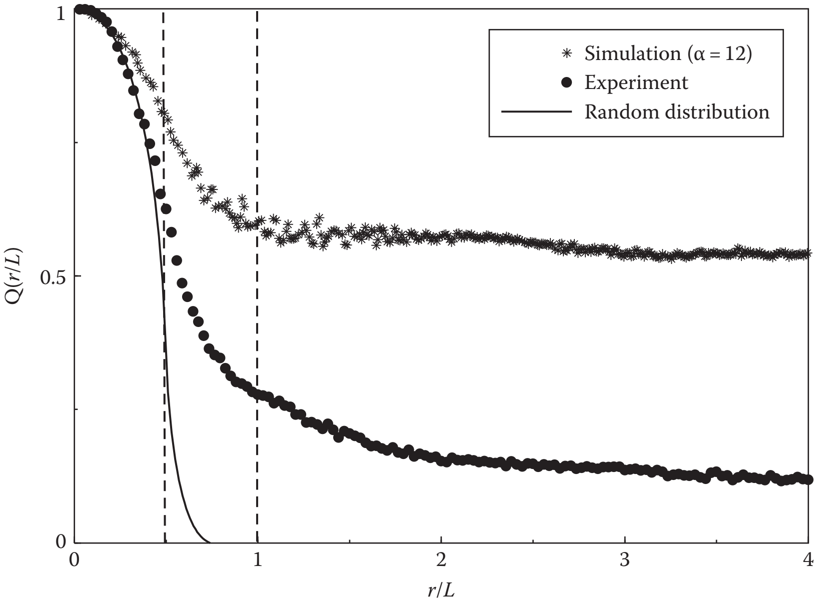

Figure 1.8 Orientational correlation function $\tilde{Q}(r/L)$ as a function of center-of-mass separation scaled by particle length. The solid line is data from an isotropic distribution, with particles assuming all allowable angles with equal probability. Both experiment (•) and simulation (∗) show an increased probability of particle alignment and (different) non-zero asymptotes for large r/L. (From Stokely, K. et al., *Phys. Rev. E.*, 67, 051302, 2003.)

pulled out of the container. Despite the absence of any other means of support, the pile maintains its original cylindrical shape and is robust to perturbations.

Because this cohesivity is caused by the particle geometry, such materials have been termed "geometrically cohesive granular materials" [18]. In these materials, the individual particle geometry enables a bulk cohesivity (as contrasted with, say, van der Waals forces in powders or capillary forces in wet materials). This behavior is most pronounced in three dimensions, as demonstrated in experiments on both long, thin rods, and radically aspherical particles (U-shaped staples). This rigidity has since been studied in the context of response to localized intruders and the collapse of columns, extending similar studies previously conducted on ordinary, round materials [1,26,27,29,30]. More recently, two systematic studies of U-shaped particles (staples) have characterized the susceptibility of piles to oscillatory disturbances and direct extensional forces.

1.3.3 Rigidity of Rodpiles

The stick-slip motion of an intruder through ordinary sand was studied by Albert et al. [1], who found force fluctuations with a characteristic $1/f^2$ scaling. Desmond and Franklin [11] repeated this experiment for rod-like materials and found three qualitatively different types of behavior. When the particle aspect ratio is low, the pile responds with local rearrangements and the drag force on the intruding

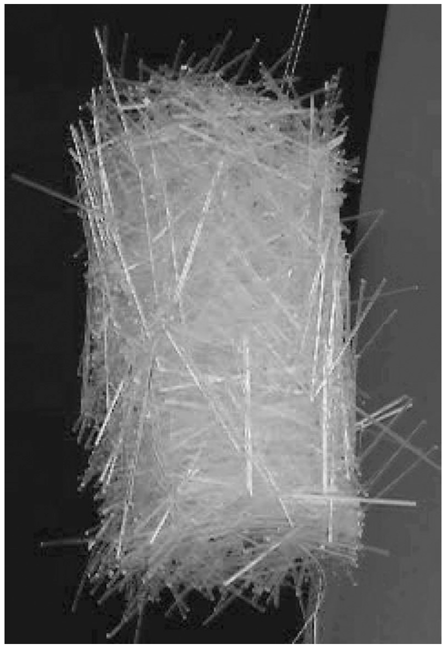

Figure 1.9 Pile of rods (aspect ratio 48) suspended by a single point force applied to the bottom. The force is applied by a single particle at the bottom which is tied to a string (exiting the pile at the top right of the image) suspended from above. The pile exhibits significant stability, resisting even large perturbing forces.

object has a random sawtooth appearance (Figure 1.10a). The linear increase in force indicates the intruder is at rest; the rapid decrease accompanies a sudden burst of motion. Importantly, the majority of the grains are at rest throughout the experiment; while individual particles near the intruder rearrange, there is no visible collective pile motion. A Fourier transform of the force vs. time data, shown in Figure 1.11, has a power-law tail that decays as f^{-2}, consistent with Albert et al.'s earlier experiments on stick-slip rearrangements in round particles.

As discovered by Philipse, piles of particles with large aspect ratios exhibit a distinct solid-like behavior. When an upward force is applied by the intruder, the pile as a whole moves upward. There is little observed relative motion between particles, and the pile acts as a solid. This behavior is reflected in the force vs. time diagram (Figure 1.10c). Two features are important to note. First, the force needed to move the pile (normalized by the total pile weight in Figure 1.10) can be many times the actual pile weight. This is a manifestation of discrete force chains [10,25] which, when deflected laterally, are amplified (see discussion earlier in this Chapter) before terminating on the container walls. The unusually large normal forces on the wall result in correspondingly large frictional forces that the force from the intruder must be overcome. The second feature to note is the spectrum of the fluctuations, shown in Figure 1.11, which has a different scaling exponent than that from granular rearrangements. The spectrum of these fluctuations decays as

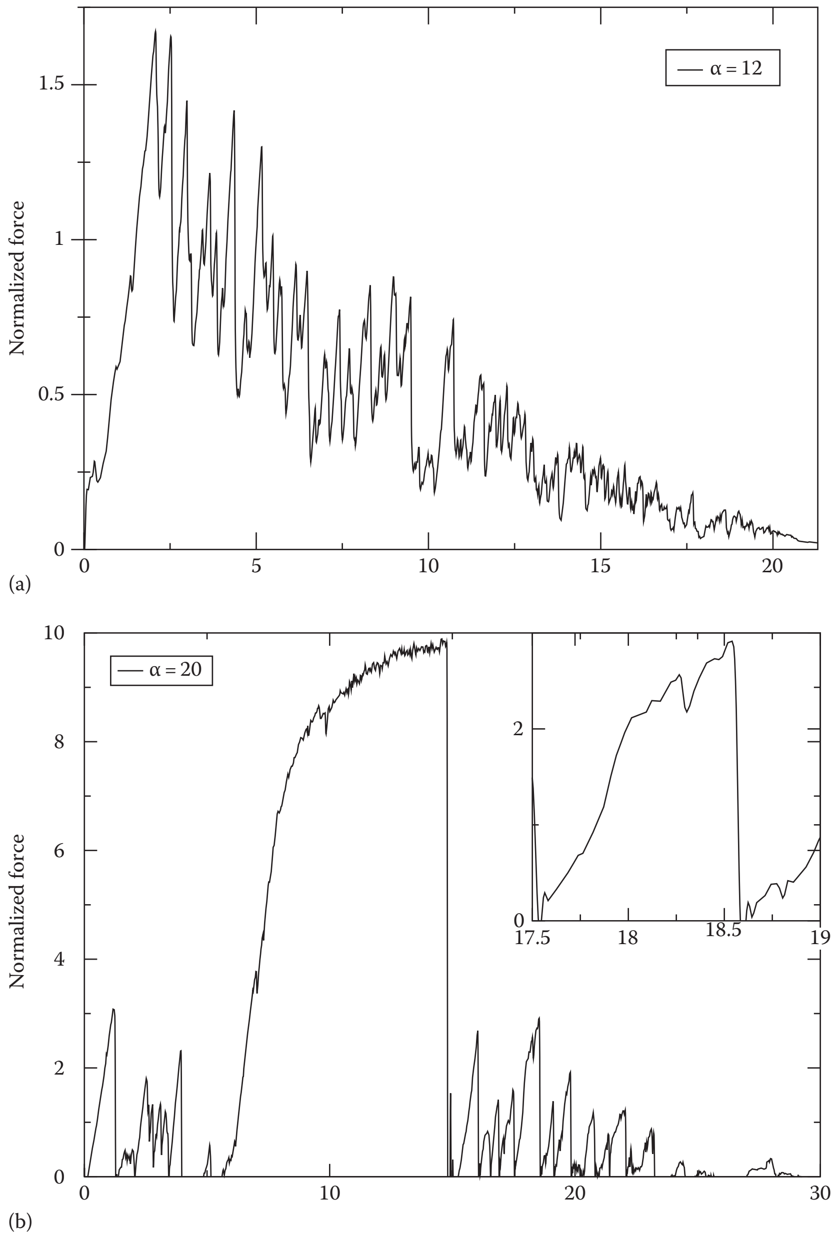

Figure 1.10 Force vs. time data for a ball dragged through a pile of rods of aspect ratio 12 (a), 20 (b), and 40 (c), all in a 5 cm tube. The low aspect ratio particles show the stick-slip behavior common in ordinary granular materials. The large aspect ratio particles, however, act as a single solid body, with small fluctuations characteristic of dry friction. Intermediate aspect ratios show both behaviors in a single experiment on both large and small (inset) time scales. (*Continued*)

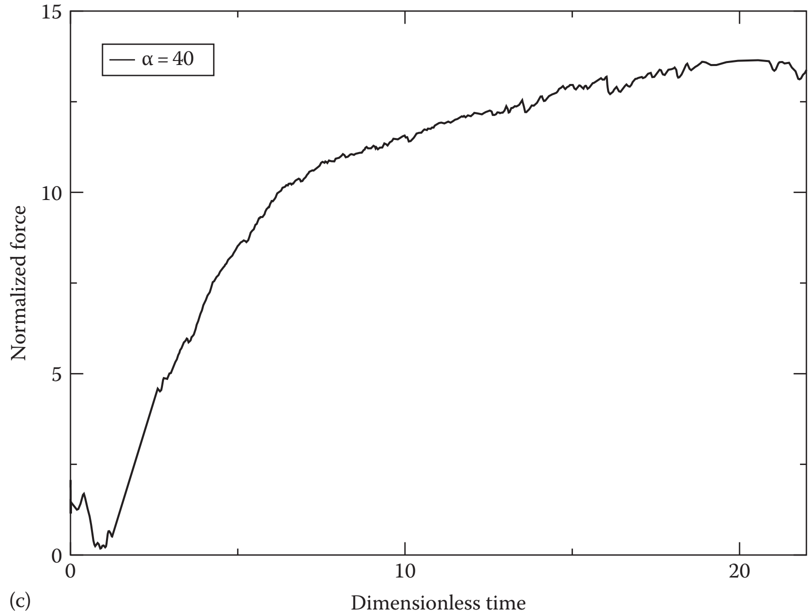

Figure 1.10 (*Continued*) Force vs. time data for a ball dragged through a pile of rods of aspect ratio 12 (a), 20 (b), and 40 (c), all in a 5 cm tube. The low aspect ratio particles show the stick-slip behavior common in ordinary granular materials. The large aspect ratio particles, however, act as a single solid body, with small fluctuations characteristic of dry friction. Intermediate aspect ratios show both behaviors in a single experiment on both large and small (inset) time scales. (From Desmond, K. and Franklin, S.V. *Physical Review E*, 73(3), 031306, March 2006.)

f^{-1}, a behavior similar to that found in ordinary dry friction (e.g., [13]), further supporting the interpretation that the resistance to motion is primarily frictional.

Desmond et al. discovered an interesting combination of granular and solid-like behaviors displayed by particles of intermediate aspect ratios. As seen in Figure 1.10b, the pile at first responds to the intruder with the characteristic stick-slip motion associated with small aspect ratio particles. A close examination of the force (inset in Figure 1.10b), however, shows that these fluctuations contain small plateaus. As plateaus correspond to more steady upward motions, these imply small periods of time in which the pile moves as a solid. The data in Figure 1.10b show a long period of time, during the middle of the experiment, when the entire pile jams and all particles above the intruder move together. During this time, the pile is visually observed to move as a solid. Unlike the large aspect ratio particles, however, this pile is not as stable to perturbations, and eventually (at around $t = 15$ s) the pile collapses around the intruder and the stick-slip behavior resumes. The length of time spent in the solid state can be interpreted as an indication of the pile's stability. A related experiment on column collapse [47] found a similar combination of granular and solid behaviors in intermediate particle aspect ratios.

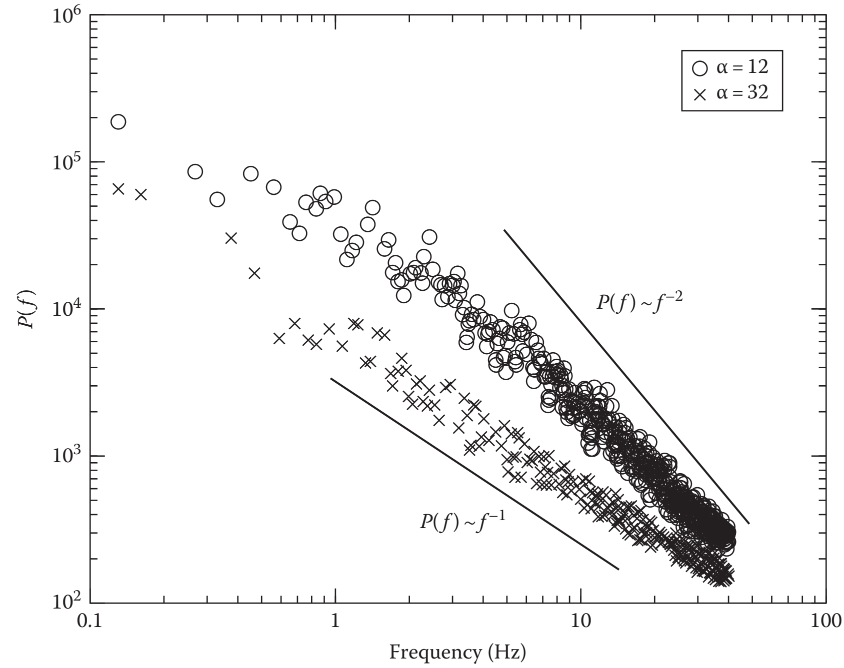

Figure 1.11 Power spectra for force fluctuations from piles exhibiting granular (○) and solid (x) behavior. Both show power-law tails, with the different exponents indicating a different mechanism for the fluctuations. The $1/f$ and and $1/f^2$ decay are consistent with previous work on, respectively, dry friction and localized granular rearrangements. Both data sets taken in a D = 2″ diameter tube. (From Desmond, K. and Franklin, S.V. *Physical Review E*, 73(3), 031306, March 2006.)

The behavior is dependent not only on the particle aspect ratio L/d but also the container diameter $\tilde{D}$. (The normalized inverse container diameter $\delta \equiv /D$ is actually used as the control parameter.) A "phase diagram" of pile behavior is shown in Figure 1.12. Figure 1.12 shows that when the aspect ratio is very small the pile behaves in a canonically granular manner. Nevertheless, the signature characteristics of the transition region plateaus in the force data and a visual observation of collective motion are seen in particles with aspect ratios as low as 8 when confined to cylinders whose diameter is twice the particle length.

1.3.4 Melting of U-Shaped Staples

U-shaped particles entangle significantly, and are considerably more solid-like than long thin rods. Gravish et al. [18] investigated the response of these particles in response to oscillatory disturbances, in the process deriving a novel characterization of rigidity. The height of a shaken pile decreased with time as a stretched exponential, introducing a time scale for the "melting." This time scale was inversely proportional to the oscillation strength (measured as the peak acceleration), and Gravish characterized rigidity by the proportionality constant of this

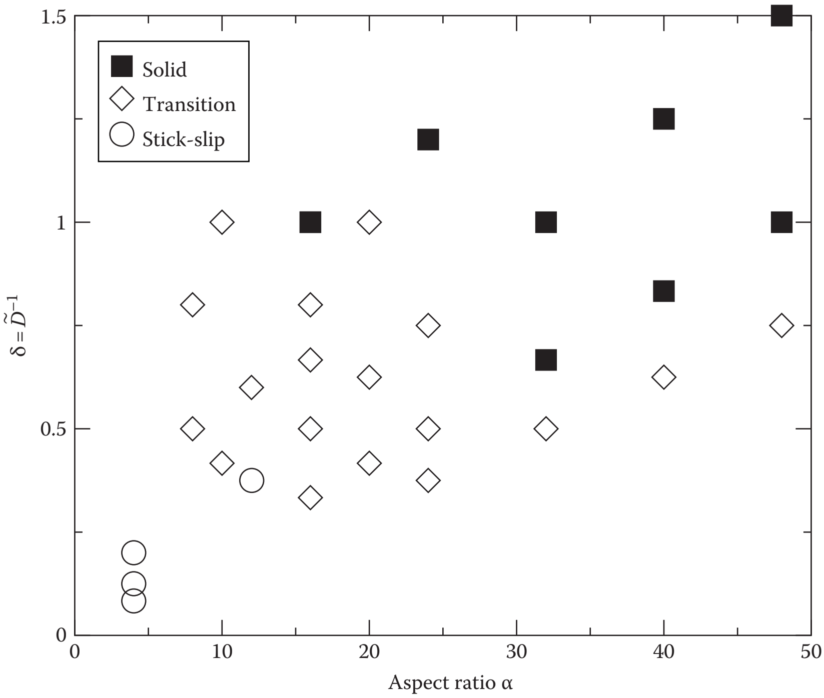

Figure 1.12 Phases exhibited by granular piles as a function of two control parameters—the aspect ratio α and the inverse container diameter $\delta \equiv \tilde{D}^{-1}$. Smaller aspect ratio particles show the stick-slip behavior of granular materials, while larger aspect ratio particles act as a solid body when the container is small enough. (From Desmond, K. and Franklin, S.V. *Physical Review E*, 73(3), 031306, March 2006.)

relationship. Figure 1.13a shows this measure as a function of the particle arm to spine "barb" ratio; first increasing, and then decreasing.

This behavior can be understood by considering the density of entanglements. An entanglement for these particles occurred when the arm of one particle passed between the arms of another. The probability of entanglement is related to the area spanned by the particle arms, and so increases with barb ratio. The particle density, however, decreases with barb ratio, similar to the behavior of large aspect ratio rods discussed earlier. The entanglement density is (roughly) proportional to the product of these two quantities. Figure 1.13b shows the entanglement density measured from Monte Carlo simulations, and reveals a peak density at approximately the same barb ratio as that maximally resistant to oscillations. Gravish et al. thus naturally concluded that rigidity is due to entanglement density, a hypothesis currently being explored in simulations.

There is a second interpretation of nonmonotonic dependence with barb ratio. As the barb ratio increases the "open" end of the particle represents a smaller fraction of the circumference. There would therefore seem to be a smaller probability of another particle finding this opening and becoming entangled. An intriguing system in which to study this would seem to be arcs of varying subtended angle.

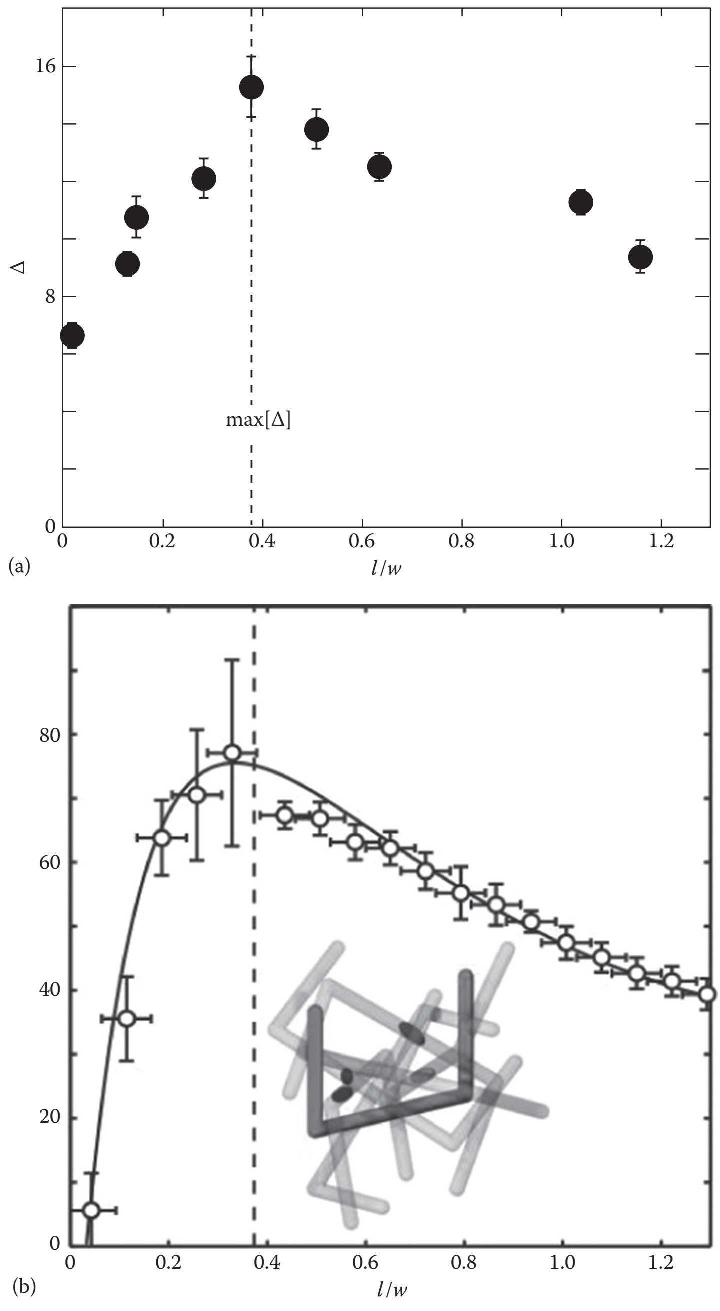

Figure 1.13 (a) Rigidity parameter (with regard to oscillation) Δ as a function of particle barb ratio l/w. Rigidity peaks when the arms are ≈40% of the spine length. (b) Entanglement density as a function of l/w from simulations and theoretical fit. The density peaks at a barb ratio comparable to that corresponding to peak rigidity. (From Gravish, N. et al. *Phys. Rev. Lett.*, 105, 128301, 2010.)

Clearly circles (subtending a full 2π radians) cannot entangle, nor are very short arcs likely to entangle in a meaningful way. This gedanken experiment would seem to recapture the maximally rigid shape without the dramatic decrease in packing fraction that the large barb ratio particles have.

1.3.5 Rheology of U-Shaped Staples

The previous sections involved experimental geometries intruder motion, column collapse, and oscillatory disturbances—originally applied to ordinary, round granular materials. We conclude with an experiment that cannot be applied to dry granular materials: extensional rheology. In an extensional test, one end of a granular sample is held fixed and the opposing end pulled with either a constant force or (attempted) constant velocity. As there are no cohesive properties in ordinary, dry granular materials, the very question of effective Young's modulus does not apply. The question only makes sense for materials that do demonstrate extensional cohesivity: granular materials that are wet, charged, or, in the case we now consider, geometrically cohesive.

The experiment consists of a cylindrical pile of U-shaped staples. Particles have a spine length of 1.3 cm and an arm length of 0.64 cm; the resulting barb ratio of $1.3/6.4 = 0.5$ is very near to that found by Gravish et al. to result in maximum entanglement. The staples, ordinary office staples, are made of wire thin enough to penetrate most voids in the pile, thus explaining the maximal entanglement. One end of the pile is held fixed; the other attached to a spring, which is then pulled with a constant speed. The instantaneous applied force and sample length can be independently measured to obtain a force-elongation curve such as Figure 1.14.

Fluctuations in Figure 1.14 are similar to those observed in response to an intruder through granular materials (e.g., [1,11]), but in this case arise due to the unsteady growth of the pile length. A yield force can be defined as the peaks in these graphs; the inset in Figure 1.14 shows peaks identified by computer analysis. Although there is a slight memory effect, with small differences in the distribution of forces that occur before and after large events, yield events can be treated as effectively independent (statistically). As a result, a single experiment effectively samples yielding at a range of pile lengths.

The most striking observation from this experiment is that longer piles are significantly weaker than shorter piles. Shown in Figure 1.15, the mean yield force decays with instantaneous sample length as a power-law with exponent $(0.86 \pm 0.12)^{-1}$. This gives a powerful clue toward the underlying mechanism, suggesting that yielding is due to a "weakest link" within the sample. Longer piles have statistically greater chances of containing a weak link and thus are more susceptible to yielding at lower applied forces.

The theory of weakest link statistics was worked out by Weibull [49] in 1939, and rests on the sole assumption that a long sample is comprised of multiple smaller elements, each with a statistically independent yielding probability. For a sample to not fail or yield, each subelement must similarly not fail. If the

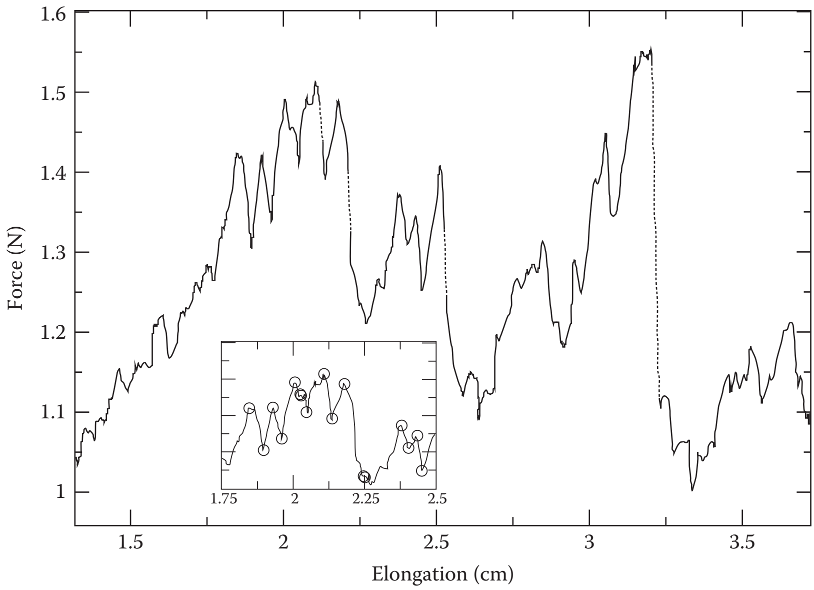

Figure 1.14 The extension of a geometrically cohesive granular material is accompanied by fluctuations in the applied force. A decrease in force implies a rapid sample growth; peaks therefore indicate yield events before a significant rearrangement. Inset shows critical points where rapid growth starts and stops identified by computer analysis. (From Franklin, S.V., *EPL*, 58004+, 2014.)

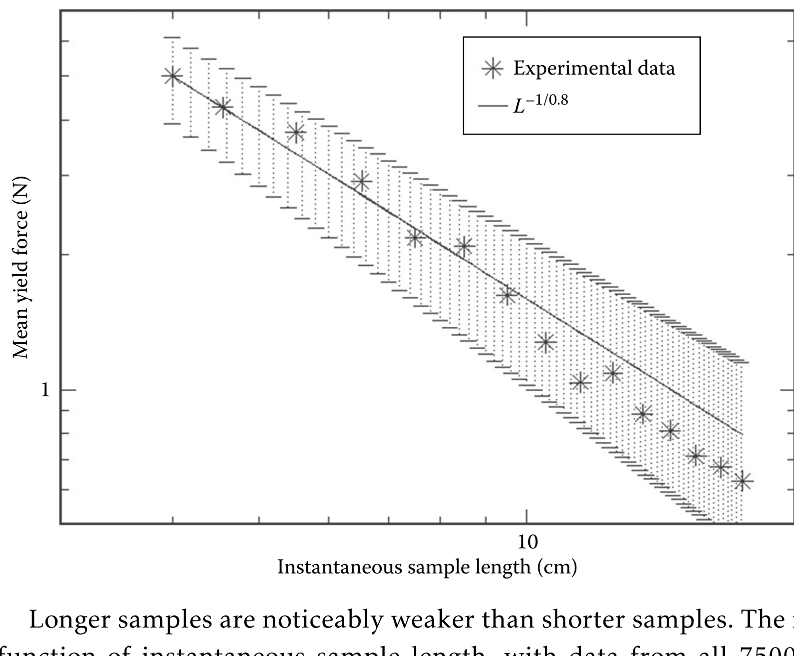

Figure 1.15 Longer samples are noticeably weaker than shorter samples. The mean yield force as a function of instantaneous sample length, with data from all 7500 identified events, shows the mean force to decay as a power-law with $L^{-1/m}$. The value of m is determined from the Weibullian analysis to be $m = 0.86 \pm 0.12$; therefore this fit has no free parameters. (Error bars represent the bounds of the power-law fit.) (From Franklin, S.V., *EPL*, 58004+, 2014.)

probability for a differential length δL to fail is $\delta Y = p(F)\delta L$, then the probability for it not to yield is $1 - \delta Y$ and the probability that the entire sample holds is

$$1 - P(F,L) = \prod_i [1 - p(F)\delta L].$$

where the product is over the N subelements.

If the probability of each subunit failing is small, this can be simplified by taking the logarithm of both sides and then Taylor expanding the resulting sum about 1:

$$\ln[1 - P(F,L)] = \sum_i \ln[1 - p(F)\delta L] \approx \sum_i \alpha p(F)\delta L$$

or, since $\sum_i \delta L = L$

$$1 - P(F,L) \approx e^{-p(F)L}.$$

$P(F,L) = 1 - e^{-p(F)L}$ is the probability that a sample of length L fails at instantaneous applied force F. In order for an experimental sample to realize that failure, however, it must first not fail at lower applied forces. Thus, the probability of actually observing failure at force F is the product of the sample not failing at lower forces and failing at that force:

$$Y(F,L) = C(L)e^{-p(F)L}\left(1 - e^{-p(F)L}\right)$$

where $C(L)$ is a normalization constant such that $\int Y(F,L)dF = 1$.

The power-law decay of mean yield force with length suggests we consider that the subunit yield probability scale similarly as a power-law with force, that is, $p(F) = F^m$. The mean force is then found by averaging over all yield forces

$$\begin{aligned}\overline{F}(L)\rangle &= \int_0^\infty FP(F,L)\, dF \\ &= CL^{1/m} \int_0^\infty F\left[e^{-\alpha ALF^m} - e^{-2\alpha ALF^m}\right] \\ &\propto L^{-1/m},\end{aligned} \tag{1.13}$$

the very power-law shown in the data in Figure 1.13.

1.4 Additional Studies

The study of irregularly shaped particles is still quite new, certainly compared to that of round particles. Still, our coverage is not meant to be a comprehensive summary of cylindrical, ellipsoidal or similarly shaped particles, and interested readers are referred to a number of interesting resources. Villarruel et al. [48] found that rods of aspect ratio ≈4 constrained to a cylinder would, when tapped, align with the cylinder walls and compact. Lumay and Vandewalle [31] extended this to still larger aspect ratios, and developed a 2D lattice model that reproduced the salient features of the compaction curves. A subsequent two-dimensional experiment highlighted the importance of rotation in rod rearrangements [32]. Pournin et al. [29,40] derived an analytic expression for detecting contact between spherocylinders (a spherocylinder is composed of a cylinder and two hemispherical endcaps), an integral component of efficient computation. A spherocylinder can be defined as the locus of points equidistant from a line segment, so the problem reduces to finding the shortest distance between two segments. Pournin et al. used these results to develop discrete element method simulations that show crystallization and ordering under various excitations.

More recently, Hidalgo et al. [20] studied the role particle shape plays on stress propagation through a granular packing, while Azema and Radjï [2] examined the stress–strain relations of rod packings under shear. Attention has also been paid to the nature of random packings. Wouterse et al. [50] characterized the microstructure of random packings of spherocylinders and Zeravcic et al. [52] looked at the excitations of random ellipsoid packings at the onset of jamming.

For review, the reader is referred to Borzsonyi et al. [6], which nicely summarizes the research on shape anisotropic or *anisometric* [35] granular materials. Here one will find results pertaining to orientational ordering, the distribution of stresses throughout the sample, shear studies and fluidization, and/or the gaseous state that accompanies vigorous input of energy. We agree with and call attention to the authors, note of the lack of quantitative experiments in 3D bulk piles. It is quite likely that, as the authors state, we may expect "surprising details" to result from more complex geometries.

1.5 Conclusion

This chapter began by reviewing several investigations—theoretical, computational, and experimental—that revealed the power of uncorrelated mean-field statistics. Many of these were seen to be analogous to some form of a random walk, and the naive assumptions in the models justified by qualitative (and sometimes quantitative) agreement with observations. No attempt was made to be comprehensive, and it should be emphasized that the understanding has evolved considerably from some of the earlier interpretations. In particular, the theory of force chain generation is not nearly as simple as originally posited in the q-model, and the reader is referred to Chapter 7 for more recent theoretical innovations. Nevertheless, each can be considered to have advanced considerably the field of granular research, and it is quite likely that similarly simple models will arise again in the future to trigger new understandings.

Moving to radically aspherical shapes such as long, thin rods, and U-shaped samples, we saw that instances where mean-field approximations began to break down. These geometries introduce experimental complexities, such as choosing an appropriate system size and defining relevant dimensionless quantities, that are only now beginning to be overcome. While computational work has contributed greatly to our understanding of these particles, experiments continue to provide new phenomena that must be understood. As the field progresses, one can imagine new work that begins to consider mixtures of particles at the same particulate level of understanding that is currently only available to more narrow distributions of particle size and shape.

References

1. I. Albert, P. Tegzes, R. Albert, J. G. Sample, A. L. Barabasi, T. Vicsek, B. Hang, and P. Schiffer. Stick-slip fluctuations in granular drag. *Physical Review E*, 64:031307, 2001.

2. E. Azéma and F. Radja"i. Stress-strain behavior and geometrical properties of packings of elongated particles. *Physical Review E*, 81(5):051304, May 2010.

3. P. Bak, C. Tang, and K. Wiesenfeld. Self-organized criticality: An explanation of the 1/f Noise. *Physical Review Letters*, 59:381, 1987.

4. I. Balberg, C. H. Anderson, S. Alexander, and N. Wagner. Excluded volume and its relation to the onset of percolation. *Physical Review B*, 30:3933, 1984.

5. W. A. Beverloo, H. A. Leniger, and J. van de Velde. The flow of granular solids through orifices. *Chemical Engineering Science*, 15(3–4):260–269, 1961.

6. T. Borzsonyi and R. Stannarius. Granular materials composed of shape-anisotropic grains. *Soft Matter*, 9:7401–7418, 2013.

7. R. L. Brown and J. C. Richards. Essays on the packing and flow of powders and bulk solids. *Principles of Powder Mechanics*. Pergamon Press, Oxford, London, 1970.

8. J. Carlson and J. Langer. Properties of earthquakes generated by fault dynamics. *Physical Review Letters*, 62(22):2632–2635, May 1989.

9. J. Choi, A. Kudrolli, and M. Z. Bazant. Velocity profile of granular flows inside silos and hoppers. *Journal of Physics: Condensed Matter*, 17(24), S2533, 2005.

10. S. N. Coppersmith, C. Heng Liu, S. Majumdar, O. Narayan, and T. A. Witten. Model for force fluctuations in bead packs. *Physical Review E*, 53:4673, 1996.

11. K. Desmond and S. V. Franklin. Jamming of three-dimensional prolate granular materials. *Physical Review E*, 73(3):031306, March 2006.

12. J. Duran. *Sands, Powders, and Grains: An Introduction to the Physics of Granular Materials*. Springer-Verlag, Duran, New York, 2000.

13. H. J. Feder and J. Feder. Self-organized criticality in a stick-slip process. *Physical Review Letters*, 66:2669, 1991.

14. S. V. Franklin. Extensional rheology of entangled granular materials. *EPL (Europhysics Letters)*, 106(5), 58004+, June 2014.

15. E. Frossard. Recent advances in the physics of their mechanical behavior and applications to engineering works, *Granular Materials in Civil Engineering.* John Wiley & Sons, pp. 35–82, 2013.

16. G. J. Gao, J. Blawzdziewicz, and C. S. O'Hern. Enumeration of distinct mechanically stable disk packings in small systems. *Philosophical Magazine*, 87(3–5):425–431, January 2007.

17. J. Geng, E. Longhi, R. P. Behringer, and D. W. Howell. Memory in two-dimensional heap experiments. *Physical Review E*, 64:060301, 2001.

18. N. Gravish, P. B. Umbanhowar, and D. I. Goldman. Force and flow transition in plowed granular media. *Physical Review Letters,*, 105(12):128301, September 2010.

19. C. Liu, S. R. Nagel, D. A. Schecter, S. N. Coppersmith, S. Majumdar, O. Narayan, and T. A. Witten. Force fluctuations in bead packs. *Science*, 269:513, 1995.

20. R. C. Hidalgo, I. Zuriguel, D. Maza, and I. Pagonabarraga. Role of particle shape on the stress propagation in granular packings. *Physical Review Letters*, 103(11):118001, September 2009.

21. D. W. Howell and R. P. Behringer. Stress fluctuations in a 2D granular couette experiment: A continuous transition. *Physical Review Letters*, 82:5241, 1999.

22. H. M. Jaeger, C. Heng Liu, and S. R. Nagel. Relaxation at the angle of repose. *Physical Review Letters*, 62:40, 1989.

23. A. Janda, I. Zuriguel, A. GarcimartÃn, L. A. Pugnaloni, and D. Maza. Jamming and critical outlet size in the discharge of a two-dimensional silo. *EPL (Europhysics Letters)*, 84(4):44002, 2008.

24. J. B. Knight, C. G. Fandrich, C. N. Lau, H. M. Jaeger, and S. R. Nagel. Density relaxation in a vibrated granular material. *Physical Review E*, 51:3957, 1995.

25. D. Kolymbas (ed). *Constitutive Modelling of Granular Materials*. Springer, Berlin, Heidelberg, 2000.

26. E. Lajeunesse, A. Mangeney-Castelnau, and J. P. Vilotte. Spreading of a granular mass on a horizontal plane. *Physics of Fluids*, 16(7):2371–2381, 2004.

27. E. Lajeunesse, J. B. Monnier, and G. M. Homsy. Granular slumping on a horizontal surface. *Physics of Fluids*, 17(10):103302, 2005.

28. P. Le Doussal, A. Middleton, and K. Wiese. Statistics of static avalanches in a random pinning landscape. *Physical Review E*, 79(5), May 2009.

29. G. L. Ad and M. A. Hallworth. Axisymmetric collapses of granular columns. *Journal of Fluid Mechanics*, 508:175, 2004.

30. G. Lube, H. E. Huppert, J. Sparks, and A. Freundt. Collapses of two-dimensional granular columns. *Physical Review E*, 72:041301, 2005.

31. G. Lumay and N. Vandewalle. Compaction of anisotropic granular materials: Experiments and simulations. *Physical Review E*, 70:051314, 2004.

32. G. Lumay and N. Vandewalle. Experimental study of the compaction dynamics for two-dimensional anisotropic granular materials. *Physical Review E*, 74:021301, 2006.

33. E. R. Nowak, J. B. Knight, E. Ben-Naim, H. M. Jaeger, and S. R. Nagel. Density fluctuations in vibrated granular materials. *Physical Review E*, 57:1971, 1998.

34. C. S. O'Hern, S. A. Langner, A. J. Liu, and S. R. Nagel. Force distributions near jamming and glass transitions. *Physical Review Letters*, 86:111, 2001.

35. L. Onsager. The effects of shape on the interaction of colloidal particles. *Annals of the New York Academy of Science*, 51:627, 1949.

36. O. Perković, K. Dahmen, and J. Sethna. Avalanches, Barkhausen noise, and plain old criticality. *Physical Review Letters*, 75(24):4528–4531, December 1995.

37. A. P. Philipse. The random contact equation and its implications for (Colloidal) rods in packings, suspensions, and anisotropic powders. *Langmuir*, 12:1127, 1996.

38. A. P. Philipse and A. Verberkmoes. Statistical geometry of caging effects in random thin-rod structures. *Physica A*, 235:186, 1997.

39. L. Pournin, M. WEber, M. Tsukahara, J. A. Ferrez, M. Ramaioli, and Th Libling. Three-dimensional distinct element simulation of spherocylinder crystallization. *Granular Matter*, 7:119, 2005.

40. M. Ramaioli, L. Pournin, and Th Liebling. Vertical ordering of rods under vertical vibration. *Physical Review E (Statistical, Nonlinear, and Soft Matter Physics)*, 76(2):021304, 2007.

41. S. Saraf and S. V. Franklin. Power-law flow statistics in anisometric (wedge) hoppers. *Physical Review E*, 83(3):030301, March 2011.

42. J. P. Sethna, K. A. Dahmen, and C. R. Myers. Crackling noise. *Nature*, 410(6825):242–250, March 2001.

43. K. Stokely, A. Diacou, and S. V. Franklin. Two-dimensional packing in prolate granular materials. *Physical Review E*, 67(5):051302, 2003.

44. K. To and P.-Y. Lai. Jamming pattern in a two-dimensional hopper. *Physical Review E*, 66:011308, 2002.

45. K. To, P.-Y. Lai, and H. K. Pak. Jamming of granular flow in a two-dimensional hopper. *Physical Review Letters*, 86:71, 2001.

46. K. To, P.-Y. Lai, and H. K. Pak. Flow and jam of granular particles in a two-dimensional hopper. *Physica A*, 315:174, 2002.

47. M. Trepanier and Scott V. Franklin. Column collapse of granular rods. *Physical Review E*, 82:011308, 2010.

48. F. X. Villarruel, B. E. Lauderdale, D. M. Mueth, and H. M. Jaeger. Compaction of rods: Relaxation and ordering in vibrated, anisotropic granular material. *Physical Review E*, 61:6914, 2000.

49. W. Weibull. A statistical theory of the strength of materials. Technical Report 151, Royal Swedish Academy of the Engineering Society, Stockholm, 1939.

50. A. Wouterse, S. R. Williams, and A. P. Philipse. Effect of particle shape on the density and microstructure of random packings. *Journal of Physics: Condensed Matter*, 19(40):406215, 2007.

51. N. Xu, J. Blawzdziewicz, and C. O'Hern. Random close packing revisited: Ways to pack frictionless disks. *Physical Review E*, 71(6):061306+, June 2005.

52. Z. Zeravcic, N. Xu, A. J. Liu, S. R. Nagel, and W. van Saarloos. Excitations of ellipsoid packings near jamming. *EPL* (*Europhysics Letters*), 87(2):26001, 2009.

53. I. Zuriguel, A. Garcimartin, D. Maza, L. A. Pugnaloni, and J. M. Pastor. Jamming during the discharge of granular matter from a silo. *Physical Review E*, 71:051303, 2005.

54. I. Zuriguel, L. A. Pugnaloni, A. Garcimartin, and D. Maza. Jamming during the discharge of grains from a silo described as a perocolating transition. *Physical Review E*, 68:030301, 2003.

Section I

Interpretive Frameworks

CHAPTER 2

Experimental Techniques

Mark D. Shattuck

CONTENTS

2.1 Introduction

From the beach to the sandbox, granular experiments begin at an early age. Even to a child, it is clear that sand behaves differently than ordinary fluids and solids. When poured, sand flows like a fluid, but it can form a pile. When stationary, it supports the weight of a person like a solid, but patterns can form on the surface like frozen ripples on water (Figure 2.1). Dissipation and purely repulsive